

Natures of Statefinder Parameters and Om Diagnostic for Cardassian Universe in Hořava-Lifshitz Gravity

Piyali Bagchi Khatua^{1*} and Ujjal Debnath^{2†}

¹*Department of Computer Sc and Engg, Netaji Subhas Engineering College, Garia, Kolkata-700 152, India.*

²*Department of Mathematics, Bengal Engineering and Science University, Shibpur, Howrah-711 103, India.*

(Dated: August 8, 2011)

In this work, we have considered Cardassian Universe in Hořava-Lifshitz gravity. Four types of Cardassian Universe models i.e., polytropic/power law, modified polytropic, exponential and modified exponential models have been considered for accelerating models. The natures of statefinder parameters, deceleration parameter, Om diagnostic and EoS parameters have been investigated for all types of Cardassian models in Hořava-Lifshitz gravity.

I. INTRODUCTION

Recent observations of the luminosity of type Ia supernovae indicate an accelerated expansion of the universe [1-7] and lead to the search for a new type of matter, called dark energy, which violates the strong energy condition [8-10]. For explaining the accelerating expansion of the universe, large number of cosmological models have been proposed. Dark energy model is proposed by assuming an energy component with negative pressure in the universe, this dark energy dominates the total energy density of the universe and drives its acceleration of expansion at recent times. Some authors have explored possible explanations for the acceleration: (i) cosmological constant, (ii) quintessence [11-17], (iii) gravitational leakage into extra dimensions [18-19]. Accelerated expansion also depends on other observations such as the cosmic microwave background (CMB) [20] and galaxy power spectra [21]. Another reason of acceleration is the geometric effect of the general relativity fails in the present cosmic time space scale. The model proposed by Freese and Lewis, called Cardassian model [22-26], assume that the universe is flat and accelerating which consists only of matter and radiation [27]. The geometry is flat as required by measurements of the cosmic background radiation, so that there are no curvature terms in the equation and no vacuum term in the equation and so the model does not address the cosmological constant. In Cardassian Model, we take $g(\rho)$ as a function of ρ that returns simply to $l^2\rho/3$ at early epochs, where $l^2 = 8\pi G_c$.

On the basis of the recent observation one can state that if Einstein's theory of gravity is acceptable on cosmological scales, then our universe must be dominated by a mysterious form of energy called dark energy. Recently Hořava [28-29] proposed a new theory of gravity, which is renormalizable with higher spatial derivatives in four dimensions which reduces to Einstein's gravity with non vanishing cosmological constant in IR but with improved UV behaviours. In Lifshitz [30] scalar field theory the time dimension has weight 3 if a space dimension has weight 1 and this theory is called Hořava-Lifshitz gravitational theory. Hořava-Lifshitz gravity has been studied and extended in detail and applied as a cosmological framework of the universe [31-33].

As so many cosmological models have been developed, so for discrimination between these contenders, Sahni et al [34] proposed a new geometrical diagnostic named the statefinder pair $\{r, s\}$, where r is generated from the scalar factor a and its derivatives with respect to the cosmic time t and s is a simple combination of r and the deceleration parameter q . Clear differences for the evolutionary trajectories in the r - s plane have been found. In this work, we have discussed four different types of Cardassian Universe models in Hořava-Lifshitz gravity. In every case we find the statefinder parameters, deceleration parameter and Om diagnostic [34-36].

II. CARDASSIAN UNIVERSE IN HOŘAVA-LIFSHITZ GRAVITY

The Arnowitt-Deser-Misner formalism of the full metric is written as [37],

* piyali.bagchi@yahoo.co.in

† ujjaldebmath@yahoo.com

$$ds^2 = -N^2 dt^2 + g_{ij}(dx^i + N^i dt)(dx^j + N^j dt) \quad (1)$$

Under the detailed balance condition the full action condition of Hořava-Lifshitz gravity is given by,

$$S = \int dt d^3x \sqrt{g} N \left[\frac{2}{\kappa^2} (K_{ij} K^{ij} - \lambda K^2) + \frac{\kappa^2}{2\omega^4} C_{ij} C^{ij} - \frac{\kappa^2 \mu \epsilon^{ijk}}{2\omega^2 \sqrt{g}} R_{il} \nabla_j R_k^l \right. \\ \left. + \frac{\kappa^2 \mu^2}{8} R_{ij} R^{ij} + \frac{\kappa^2 \mu^2}{8(3\lambda - 1)} \left(\frac{1 - 4\lambda}{4} R^2 + \Lambda R - 3\Lambda^2 \right) \right] \quad (2)$$

where the extrinsic curvature and Cotton tensor is defined as, $K_{ij} = \frac{1}{2N}(\dot{g}_{ij} - \nabla_i N_j - \nabla_j N_i)$ and $C^{ij} = \frac{\epsilon^{ijkl}}{\sqrt{g}} \nabla_k (R_l^j - \frac{1}{4} R \delta_l^j)$. The covariant derivatives are defined w.r.t. the spatial metric g_{ij} . ϵ^{ijk} is the totally antisymmetric unit tensor, λ is a dimensionless coupling constant and the variable κ , ω and μ are constants with mass dimensions -1 , 0 , 1 respectively. Also Λ is a positive constant, which as usual is related to the cosmological constant in the IR limit.

Now, in order to focus on cosmological frameworks, we impose the so called projectability condition and use a Friedmann-Robertson-Walker (FRW) metric we get, $N = 1, g_{ij} = a^2(t) \gamma_{ij}, N^i = 0$ with $\gamma_{ij} dx^i dx^j = \frac{dr^2}{1 - kr^2} + r^2 d\Omega_2^2$ where $k = 0, -1, +1$ corresponding to flat, open and closed respectively. By varying N and g_{ij} , we obtain the non-vanishing equations of motions:

$$H^2 = \frac{\kappa^2}{6(3\lambda - 1)} \rho + \frac{\kappa^2}{6(3\lambda - 1)} \left[\frac{3\kappa^2 \mu^2 k^2}{8(3\lambda - 1)a^4} + \frac{3\kappa^2 \mu^2 \Lambda^2}{8(3\lambda - 1)} \right] - \frac{\kappa^4 \mu^2 k \Lambda}{8(3\lambda - 1)^2 a^2} \quad (3)$$

and

$$\dot{H} + \frac{3}{2} H^2 = -\frac{\kappa^2}{4(3\lambda - 1)} p - \frac{\kappa^2}{4(3\lambda - 1)} \left[\frac{\kappa^2 \mu^2 k^2}{8(3\lambda - 1)a^4} - \frac{3\kappa^2 \mu^2 \Lambda^2}{8(3\lambda - 1)} \right] - \frac{\kappa^4 \mu^2 k \Lambda}{16(3\lambda - 1)^2 a^2} \quad (4)$$

where $H \equiv \frac{\dot{a}}{a}$ is the Hubble parameter. Here G_c and G is defined as, $G_c = \frac{\kappa^2}{16\pi(3\lambda - 1)}$ and $G = \frac{\kappa^2}{32\pi}$ where G_c is the ‘‘cosmological’’ Newton’s constant and G is the ‘‘gravitational’’ Newton’s constant.

We can re-write the above equations as [38],

$$H^2 + \frac{k}{a^2} = \frac{l^2 \rho}{3} + \frac{k^2}{2\Lambda a^4} + \frac{\Lambda}{2} \quad (5)$$

and

$$\dot{H} + \frac{3}{2} H^2 + \frac{k}{2a^2} = -\frac{l^2 p}{2} - \frac{k^2}{4\Lambda a^4} + \frac{3\Lambda}{4} \quad (6)$$

Here, ρ and p are respectively the energy density and pressure of the universe, $l^2 = 8\pi G_c$ and choosing $8\pi G = 1$.

Freese and Lewis [22] constructed Cardassian universe models so that, in Cardassian models the universe is flat and accelerating, and yet contains only matter (baryonic or not) and radiation. The above equation governing the expansion of the universe is modified to,

$$H^2 + \frac{k}{a^2} = \frac{l^2 g(\rho)}{3} + \frac{k^2}{2\Lambda a^4} + \frac{\Lambda}{2} \quad (7)$$

which gives,

$$H = \sqrt{-\frac{k}{a^2} + \frac{l^2 g(\rho)}{3} + \frac{k^2}{2\Lambda a^4} + \frac{\Lambda}{2}} \quad (8)$$

where ρ is the total energy density of matter and radiation and we will neglect the contribution of radiation for the late-time evolution of the universe. The function $g(\rho)$ reduces to ρ in the early universe. Now,

$$g(\rho) = \rho_m + \rho_c \quad \text{and} \quad p = p_m + p_c \quad (9)$$

where ρ_m and ρ_c are the energy densities of matter and Cardassian term of the universe respectively and p_m and p_c are the pressure of matter and Cardassian term of the universe respectively. For any suitable Cardassian model, the following requirements that should be fulfilled. (i) The function $g(\rho)$ should returns to the usual form of ρ at early epochs in order to recover the thermal history of the standard cosmological. (ii) $g(\rho)$ should takes a different form at late times when $z \sim \mathcal{O}(1)$ in order to drive an accelerated expansion as indicated by the observation of SNeIa. (iii) The classical solution of the expansion should be stable, and the sound speed c_s^2 of classical perturbations of the total cosmological fluid around homogeneous FRW solutions cannot be negative.

In order to guarantee the classical solution of the expansion is stable, the sound speed c_s^2 of classical perturbations of the total cosmological fluid around homogeneous FRW solutions should always be greater than zero. If the expansion of the universe is adiabatic, the sound speed of total cosmological fluid can be represented by,

$$c_s^2 = \frac{\partial p}{\partial \rho} \quad (10)$$

Now the matter conservation equation gives,

$$\dot{\rho}_m + 3H(\rho_m + p_m) = 0 \quad (11)$$

and total fluid conservation equation gives,

$$\dot{g(\rho)} + 3H(g(\rho) + p) = 0 \quad (12)$$

From the above two equations we get,

$$\dot{\rho}_c + 3H(\rho_c + p_c) = 0 \quad (13)$$

From where we get,

$$p_c = (\rho_m + p_m) \frac{\partial g(\rho)}{\partial \rho_m} - g(\rho) - p_m \quad (14)$$

and

$$p = p_m + p_c = (\rho_m + p_m) \frac{\partial g(\rho)}{\partial \rho_m} - g(\rho) = \rho_m(1 + w_m) \frac{\partial g(\rho)}{\partial \rho_m} - g(\rho) \quad (15)$$

Now for dark matter $p_m = w_m \rho_m$, combining this with (11) we get,

$$\rho_m = \rho_0 a^{-3(1+w_m)} \quad \text{and} \quad p_m = \rho_0 w_m a^{-3(1+w_m)} \quad (16)$$

where ρ_0 be the integrating constant. Now the relation between scale factor a and the redshift z is given by $a = 1/(1+z)$ i.e. $z = (1/a) - 1$, and we replace all a by z , where value of z is taken $z \geq -1$.

III. STATEFINDER DIAGNOSTICS, DECELERATION PARAMETER AND Om DIAGNOSTIC

The flat Friedmann model which is analyzed in terms of the statefinder parameters. The trajectories in the $\{r, s\}$ plane of different cosmological models shows different behavior. The statefinder diagnostic of SNAP observations used to discriminate between different dark energy models. The statefinder diagnostic pair is constructed from the scale factor $a(t)$. The statefinder diagnostic pair is denoted as $\{r, s\}$ and defined as [34],

$$r = \frac{\ddot{a}}{aH^3} \quad \text{and} \quad s = \frac{r-1}{3(q-\frac{1}{2})} \quad (17)$$

where q is the deceleration parameter given by, $q = -\frac{a\ddot{a}}{\dot{a}^2}$. If universe is present with dark matter then the parameters can be expressed as,

$$r = 1 + \frac{9}{2(\rho_c + \rho_m)} \left(\frac{\partial p_c}{\partial \rho_c}(\rho_c + p_c) + \frac{\partial p_m}{\partial \rho_m}(\rho_m + p_m) \right) \quad (18)$$

$$s = \frac{1}{(p_c + p_m)} \left(\frac{\partial p_c}{\partial \rho_c}(\rho_c + p_c) + \frac{\partial p_m}{\partial \rho_m}(\rho_m + p_m) \right) \quad (19)$$

and

$$q = \frac{1}{2} + \frac{3}{2} \left(\frac{p_c + p_m}{\rho_c + \rho_m} \right) \quad (20)$$

As a complementary to $\{r, s\}$, a new diagnostic called Om has been recently proposed, which helps to distinguish the present matter density contrast in different models more effectively. The new diagnostic of dark energy Om is introduced to differentiate Λ CDM from other DE models. Om diagnostic is defined as [35],

$$Om(z) = \frac{\left(\frac{H(z+1)}{H_0} \right)^2 - 1}{(z+1)^3 - 1} \quad (21)$$

Thus Om involves only the first derivative of the scale factor through the Hubble parameter and is easier to reconstruct from observational data. Om is a constant in Λ CDM model, since it is independent of redshift z and it provides a null test of cosmological constant. Om diagnostic can distinguish DE models with less dependence on matter density relative to the EOS of DE.

IV. DIFFERENT MODELS OF CARDASSIAN UNIVERSE

A. Polytropic/Power Law Model (PL)

The simplest model is the power law (PL) Cardassian model where $g(\rho) = \rho + B\rho^n$, with B and $n < 2/3$ are two constants and the additional term ρ^n satisfies many observational constraints such as if the first Doppler peak of the CMB is slightly shifted, the universe is rather older, and the early structure formation $z > 1$ is unaffected. In this model $g(\rho)$ is defined as [23],

$$g(\rho) = \rho_m \left[1 + \left(\frac{\rho_m}{\rho_{card}} \right)^{(n-1)} \right] \quad (22)$$

where ρ_{card} is a characteristic constant energy density and n is a dimensionless positive constants. So from (9), (14), (16) and (22) we get,

$$\rho_c = \frac{\rho_0^n (1+z)^{3n(1+w_m)}}{\rho_{card}^{(n-1)}} \quad (23)$$

and

$$p_c = \frac{(n + nw_m - 1)\rho_0^n (1+z)^{3n(1+w_m)}}{\rho_{card}^{(n-1)}} \quad (24)$$

So the equation of states are given by,

$$w_c = \frac{p_c}{\rho_c} = (n + nw_m - 1) \quad (25)$$

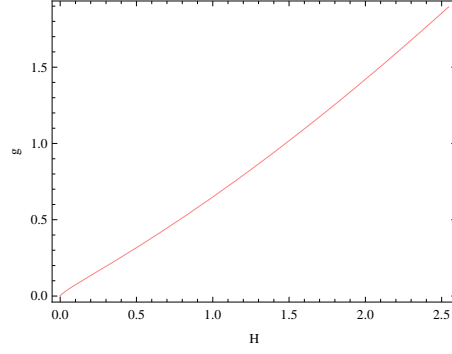


FIG. 1: The variation of g against H for $w_m = .01, n = .5, \rho_{card} = .1, \Lambda = .01, \rho_0 = .001, k = 1, l = .9, H_0 = 72$.

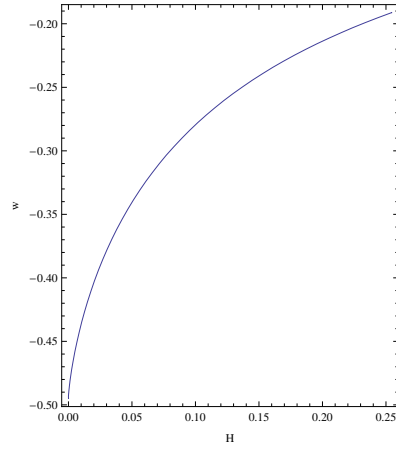


FIG. 2: The variation of w against H for $w_m = .01, n = .5, \rho_{card} = .1, \Lambda = .01, \rho_0 = .001, k = 1, l = .9, H_0 = 72$.

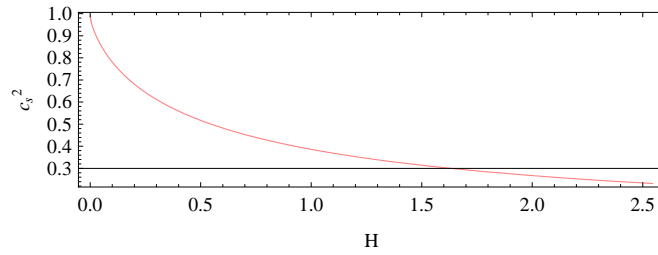


FIG. 3: The variation of c_s^2 against H for $w_m = .01, n = .5, \rho_{card} = .1, \Lambda = .01, \rho_0 = .001, k = 1, l = .9, H_0 = 72$.

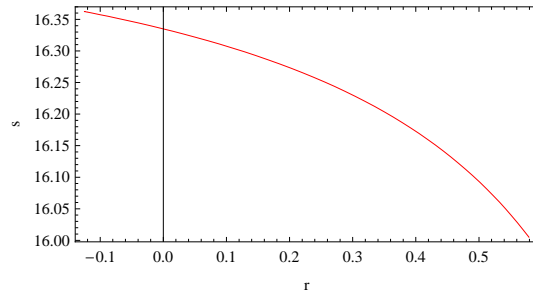


FIG. 4: The variation of s against r for $w_m = .01, n = .5, \rho_{card} = .1, \Lambda = .01, \rho_0 = .001, k = 1, l = .9, H_0 = 72$.

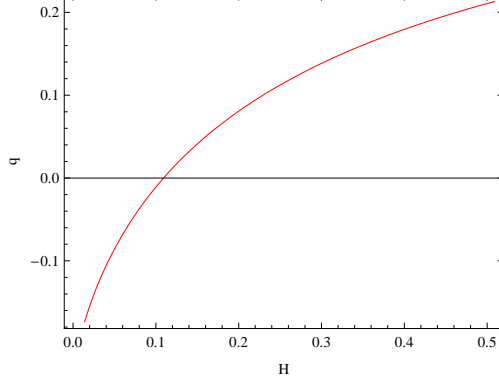


FIG. 5: The variation of q against H for $w_m = .01, n = .5, \rho_{card} = .1, \Lambda = .01, \rho_0 = .001, k = 1, l = .9, H_0 = 72$.

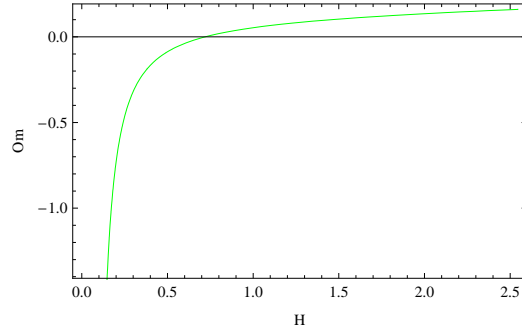


FIG. 6: The variation of Om against H for $w_m = .01, n = .5, \rho_{card} = .1, \Lambda = .01, \rho_0 = .001, k = 1, l = .9, H_0 = 72$.

and

$$w = \frac{p}{g(\rho)} = \frac{w_m + (n + nw_m - 1) \left(\frac{\rho_0(1+z)^{3(1+w_m)}}{\rho_{card}} \right)^{(n-1)}}{1 + \left(\frac{\rho_0(1+z)^{3(1+w_m)}}{\rho_{card}} \right)^{(n-1)}} \quad (26)$$

From above, we see that w_c is a constant. From (16), (18), (19), (20), (23) and (24) we get the statefinder parameters and deceleration parameter,

$$r = \frac{(1+z)^3 \rho_0 (2 + 9w_m(1+w_m)) + (1+z)^{-3w_m} \left(\frac{(1+z)^{3(1+w_m)} \rho_0}{\rho_{card}} \right)^n \rho_{card} (2 + 9n(1+w_m)(-1+n+nw_m))}{2(1+z)^3 \rho_0 + 2(1+z)^{-3w_m} \left(\frac{(1+z)^{3(1+w_m)} \rho_0}{\rho_{card}} \right)^n \rho_{card}} \quad (27)$$

and

$$s = \frac{(1+z)^3 \rho_0 w_m (11 + 9w_m) + (1+z)^{-3w_m} \left(\frac{(1+z)^{3(1+w_m)} \rho_0}{\rho_{card}} \right)^n \rho_{card} (-1+n+nw_m)(2+9n(1+w_m))}{2(1+z)^3 \rho_0 w_m + 2(1+z)^{-3w_m} \left(\frac{(1+z)^{3(1+w_m)} \rho_0}{\rho_{card}} \right)^n \rho_{card} (-1+n+nw_m)} \quad (28)$$

$$q = \frac{(1+z)^3 \rho_0 (1 + 3w_m) + (1+z)^{-3w_m} \left(\frac{(1+z)^{3(1+w_m)} \rho_0}{\rho_{card}} \right)^n \rho_{card} (-2 + 3n(1+w_m))}{2(1+z)^3 \rho_0 + 2(1+z)^{-3w_m} \left(\frac{(1+z)^{3(1+w_m)} \rho_0}{\rho_{card}} \right)^n \rho_{card}} \quad (29)$$

Fig.1 represents the variation of g against H , Fig.2 represents the variation of w against H . From (9), (10), (16), (23) and (24) we plot the graph which shows the variation of the square of velocity of sound c_s^2 against H is given in Fig.3. Fig.4 represents the variation of s against r and Fig.5 represents the variation of q against

H . From (8), (21) and (22) we get the value of Om . Fig.6 represents the variation of Om against H . The values are taken as, $w_m = .01, n = .5, \rho_{card} = .1, \Lambda = .01, \rho_0 = .001, k = 1, l = .9, H_0 = 72$. From the figures, we see that g, w, q and Om decrease as H decreases and c_s^2 lies between 0 and 1. The parameter s increases and keeps positive sign as r decreases from positive to negative values.

B. Modified Polytropic Model (MP)

Modified polytropic Cardassian model is a slight modification of the previous one, can be used on all scales, but it does not quite fit the criteria of the Cardassian model as defined above. At late times in the future of the Universe, when $\rho_m \ll \rho_{card}$, this model becomes cosmological constant dominated with $\Lambda = \rho_{card}$. This energy density is very similar to a model which motivated by gravitational leakage into extra dimensions. In this model $g(\rho)$ is defined as [25],

$$g(\rho) = \rho_m \left[1 + \left(\frac{\rho_{card}}{\rho_m} \right)^{\alpha(n-1)} \right]^{\frac{1}{\alpha}} \quad (30)$$

where ρ_{card} is a characteristic constant energy density and $\alpha \neq 0$ and n are dimensionless positive constants. So from (9), (14), (16) and (30) we get,

$$\rho_c = (1+z)^{3(1+w_m)} \rho_0 (-1 + (1 + X_{MP})^{\frac{1}{\alpha}}) \quad (31)$$

and

$$p_c = (1+z)^{3(1+w_m)} \rho_0 (X_{MP}(1 + X_{MP})^{-1+\frac{1}{\alpha}} - w_m + (1 + X_{MP})^{-1+\frac{1}{\alpha}} (w_m - X_{MP}(n + (-2+n)w_m))) \quad (32)$$

where,

$$X_{MP} = \left[\frac{(1+z)^{-3(1+w_m)} \rho_{card}}{\rho_0} \right]^{(n-1)\alpha}$$

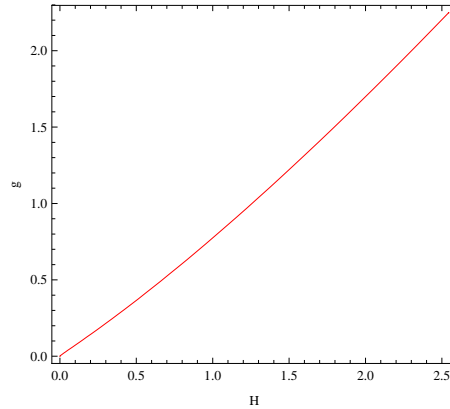


FIG. 7: The variation of g against H for $\alpha = .5, w_m = .01, n = .5, \rho_{card} = .1, \Lambda = .01, \rho_0 = .001, k = 1, l = .9, H_0 = 72$.

So the equation of state is given by,

$$w_c = \frac{(1+z)^{3(1+w_m)} \rho_0 (X_{MP}(1 + X_{MP})^{-1+\frac{1}{\alpha}} - w_m + (1 + X_{MP})^{-1+\frac{1}{\alpha}} (w_m - X_{MP}(n + (-2+n)w_m)))}{(1+z)^{3(1+w_m)} \rho_0 (-1 + (1 + X_{MP})^{\frac{1}{\alpha}})} \quad (33)$$

and

$$w = \frac{\rho_0 w_m (1+z)^{3(1+w_m)} + (1+z)^{3(1+w_m)} \rho_0 (X_{MP}(1 + X_{MP})^{-1+\frac{1}{\alpha}} - w_m + (1 + X_{MP})^{-1+\frac{1}{\alpha}} (w_m - X_{MP}(n + (-2+n)w_m)))}{\rho_0 (1+z)^{3(1+w_m)} + (1+z)^{3(1+w_m)} \rho_0 (-1 + (1 + X_{MP})^{\frac{1}{\alpha}})} \quad (34)$$

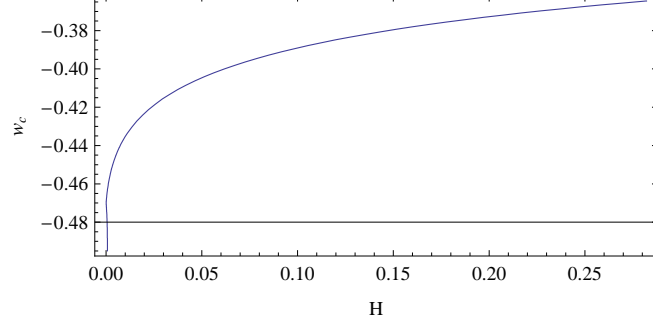


FIG. 8: The variation of w_c against H for $\alpha = .5, w_m = .01, n = .5, \rho_{card} = .1, \Lambda = .01, \rho_0 = .001, k = 1, l = .9, H_0 = 72$.

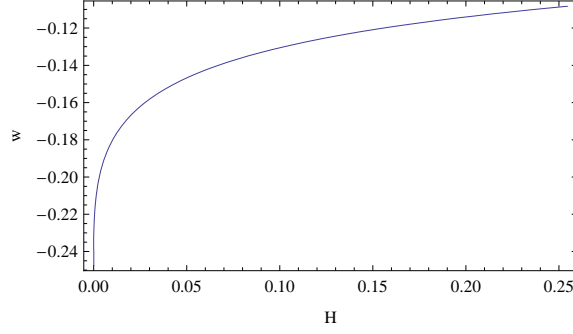


FIG. 9: The variation of w against H for $\alpha = .5, w_m = .01, n = .5, \rho_{card} = .1, \Lambda = .01, \rho_0 = .001, k = 1, l = .9, H_0 = 72$.

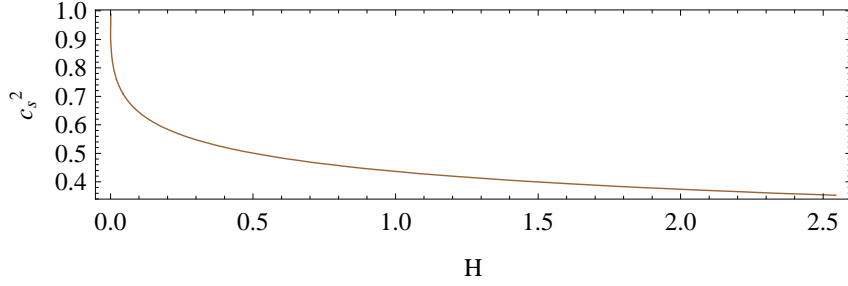


FIG. 10: The variation of c_s^2 against H for $\alpha = .5, w_m = .01, n = .5, \rho_{card} = .1, \Lambda = .01, \rho_0 = .001, k = 1, l = .9, H_0 = 72$.

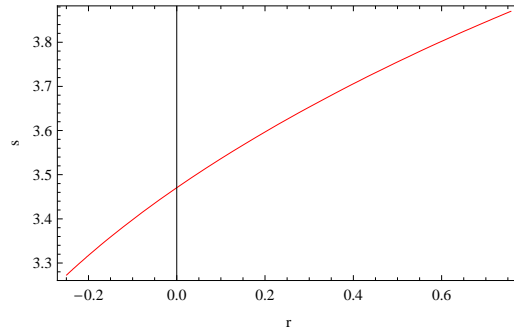


FIG. 11: The variation of s against r for $\alpha = .5, w_m = .01, n = .5, \rho_{card} = .1, \Lambda = .01, \rho_0 = .001, k = 1, l = .9, H_0 = 72$.

From (16), (18), (19), (20), (31) and (32) we get the statefinder parameters and deceleration parameter,

$$r = [2 + 9w_m + 9w_m^2 + X_{MP}(-5 - 6w_m + 3n(1 + w_m))(-4 - 6w_m + 3n(1 + w_m)) + X_{MP}(13 + 9\alpha(1 + w_m)^2]$$

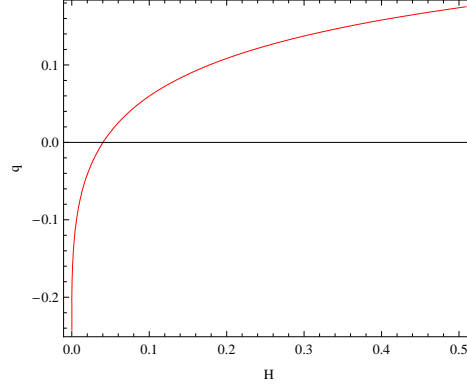


FIG. 12: The variation of q against H for $\alpha = .5, w_m = .01, n = .5, \rho_{card} = .1, \Lambda = .01, \rho_0 = .001, k = 1, l = .9, H_0 = 72$.

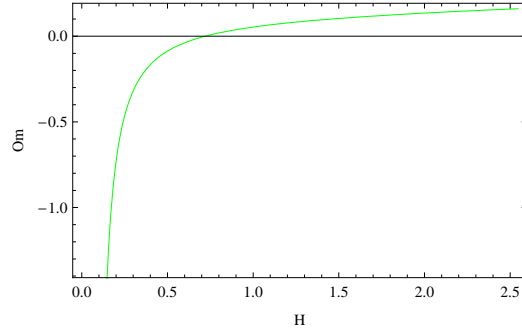


FIG. 13: The variation of Om against H for $\alpha = .5, w_m = .01, n = .5, \rho_{card} = .1, \Lambda = .01, \rho_0 = .001, k = 1, l = .9, H_0 = 72$.

$$+9n^2\alpha(1+w_m)^2 + 9w_m(5+4w_m) - 9n(1+w_m)(1+2w_m+2\alpha(1+w_m)))] / [2(1+X_{MP})^2] \quad (35)$$

and

$$s = \frac{1}{2} \left[20 - 9n + 18w_m - 9nw_m - \frac{9(-1+n)(-1+\alpha)(1+w_m)}{1+X_{MP}} - \frac{9(-1+n)\alpha w_m(1+w_m)}{-w_m + X_{MP}(-1+n+(-2+n)w_m)} \right] \quad (36)$$

$$q = \frac{1}{2} \left[4 - 3n + 6w_m - 3nw_m + \frac{3(-1+n)(1+w_m)}{1+X_{MP}} \right] \quad (37)$$

Fig.7, 8 and 9 represents the variation of g , w_c and w against H respectively. From (9), (10), (16), (31) and (32) we plot the graph which shows the variation of the square of velocity of sound c_s^2 against H is given in Fig. 10, Fig.11 represents the variation of s against r and Fig.12 represents the variation of q against H . From (8), (21) and (30) we get the value of Om . Fig.13 represents the variation of Om against H . The value of parameters are taken as, $\alpha = .5, w_m = .01, n = .5, \rho_{card} = .1, \Lambda = .01, \rho_0 = .001, k = 1, l = .9, H_0 = 72$. From the figures, we see that g, w_c, w, q and Om decrease as H decreases and c_s^2 lies between 0 and 1. The parameter s decreases and keeps positive sign as r decreases from positive to negative values.

C. Exponential Model:-

In this model $g(\rho)$ is defined as [26],

$$g(\rho) = \rho_m \exp \left[\left(\frac{\rho_{card}}{\rho_m} \right)^n \right] \quad (38)$$

where ρ_{card} is a characteristic constant energy density and n is a dimensionless positive constants. So from (9), (14), (16) and (38) we get,

$$\rho_c = (-1 + e^{X_{Exp}})(1+z)^{3(1+w_m)}\rho_0 \quad (39)$$

and

$$p_c = -(1+z)^{3(1+w_m)}\rho_0(w_m + e^{X_{Exp}}(-w_m + nX_{Exp}(1+w_m))) \quad (40)$$

where,

$$X_{Exp} = \left[\frac{(1+z)^{-3(1+w_m)}\rho_{card}}{\rho_0} \right]^n$$

So the equation of state is given by,

$$w_c = \frac{-(1+z)^{3(1+w_m)}\rho_0(w_m + e^{X_{Exp}}(-w_m + nX_{Exp}(1+w_m)))}{(-1 + e^{X_{Exp}})(1+z)^{3(1+w_m)}\rho_0} \quad (41)$$

and

$$w = \frac{\rho_0 w_0 (1+z)^{3(1+w_m)} - (1+z)^{3(1+w_m)}\rho_0(w_m + e^{X_{Exp}}(-w_m + nX_{Exp}(1+w_m)))}{\rho_0(1+z)^{3(1+w_m)} + (-1 + e^{X_{Exp}})(1+z)^{3(1+w_m)}\rho_0} \quad (42)$$

From (16), (18), (19), (20), (39) and (40) we get the statefinder parameters and deceleration parameter,

$$r = \frac{1}{2} (2 + 9w_m + 9(w_m^2 + n^2 X_{Exp}^2 (1+w_m)^2 + nX_{Exp}(1+w_m)(-1 + n + (-2 + n)w_m))) \quad (43)$$

and

$$s = \frac{1}{2} \left(11 - 9n + 9w_m - 9nw_m - 9nX_{Exp}(1+w_m) - \frac{9nw_m(1+w_m)}{-w_m + nX_{Exp}(1+w_m)} \right) \quad (44)$$

$$q = \frac{1}{2} [1 + 3w_m - 3nX_{Exp}(1+w_m)] \quad (45)$$

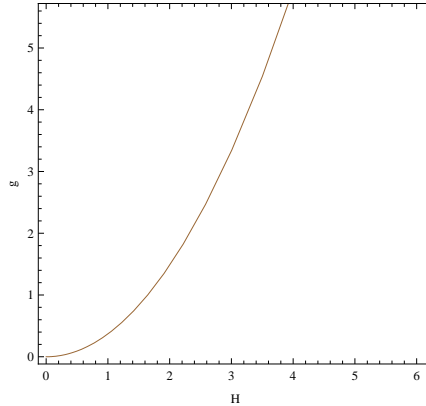


FIG. 14: The variation of w against H for $w_m = .01, n = 2, \rho_{card} = .1, \Lambda = .01, \rho_0 = .001, k = 1, l = .9, H_0 = 72$.

Fig.14, 15 and 16 represents the variation of g , w_c and w against H , z and z respectively. From (9), (10), (16), (39) and (40) we plot the graph which shows the variation of the square of velocity of sound c_s^2 against H is given in Fig. 17. Fig.18 represents the variation of s against r and Fig.19 represents the variation of q against H . From (8), (21) and (38) we get the value of Om . Fig.20 represents the variation of Om against H . The values are taken as, $w_m = .01, n = 2, \rho_{card} = .1, \Lambda = .01, \rho_0 = .001, k = 1, l = .9, H_0 = 72$. From the figures, we see that g, w_c, w, q and Om decrease as H decreases and c_s^2 lies between 0 and 1. The parameter s increases and keeps negative sign as r decreases.

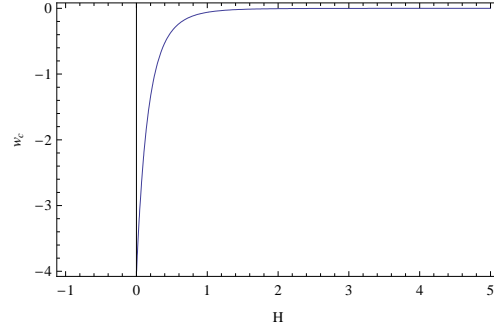


FIG. 15: The variation of w against z for $w_m = .01, n = 2, \rho_{card} = .1, \Lambda = .01, \rho_0 = .001, k = 1, l = .9, H_0 = 72$.

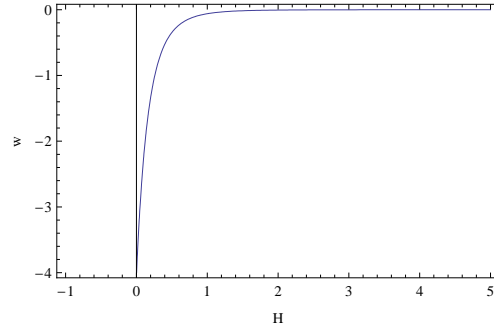


FIG. 16: The variation of w against z for $w_m = .01, n = 2, \rho_{card} = .1, \Lambda = .01, \rho_0 = .001, k = 1, l = .9, H_0 = 72$.

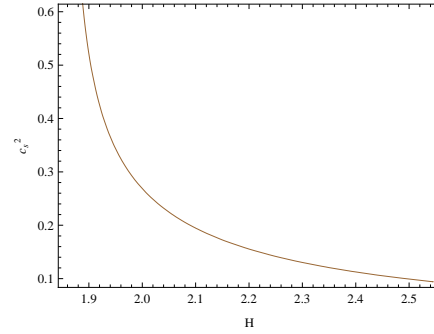


FIG. 17: The variation of c_s^2 against H for $w_m = .01, n = 2, \rho_{card} = .1, \Lambda = .01, \rho_0 = .001, k = 1, l = .9, H_0 = 72$.

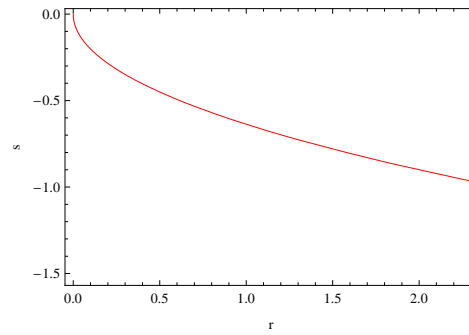


FIG. 18: The variation of s against r for $w_m = .01, n = 2, \rho_{card} = .1, \Lambda = .01, \rho_0 = .001, k = 1, l = .9, H_0 = 72$.

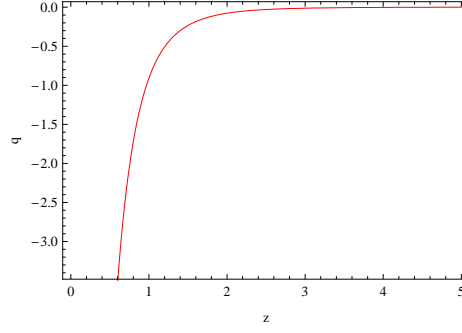


FIG. 19: The variation of q against z for $w_m = .01, n = 2, \rho_{card} = .1, \Lambda = .01, \rho_0 = .001, k = 1, l = .9, H_0 = 72$.

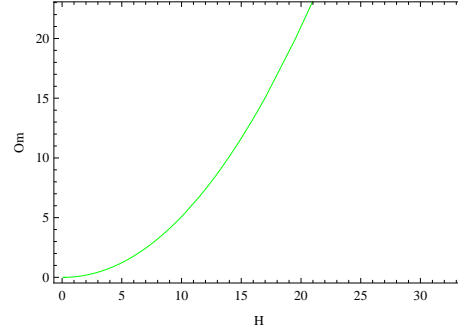


FIG. 20: The variation of Om against H for $w_m = .01, n = 2, \rho_{card} = .1, \Lambda = .01, \rho_0 = .001, k = 1, l = .9, H_0 = 72$.

D. Modified Exponential Model

In this model $g(\rho)$ is defined as [26],

$$g(\rho) = (\rho_m + \rho_{card}) \exp \left[\left(\frac{\alpha \rho_{card}}{\rho_m + \rho_{card}} \right)^n \right] \quad (46)$$

where ρ_{card} is a characteristic constant energy density and α and n are dimensionless positive constants. So from (9), (14), (16) and (46) we get,

$$\rho_c = -(1+z)^{3(1+w_m)} \rho_0 + e^{\left(\frac{\alpha \rho_{card}}{(1+z)^{3(1+w_m)} \rho_0 + \rho_{card}} \right)^n} ((1+z)^{3(1+w_m)} \rho_0 + \rho_{card}) \quad (47)$$

and

$$p_c = (1+z)^{3w_m} (-(1+z)^3 \rho_0 w_m - e^{X_{ME}} ((1+z)^{-3w_m} \rho_{card} + (1+z)^3 \rho_0 (-w_m + n X_{ME})^n (1+w_m))) \quad (48)$$

So the equation of state is given by,

$$w_c = \frac{(1+z)^{3w_m} (-(1+z)^3 \rho_0 w_m - e^{X_{ME}} ((1+z)^{-3w_m} \rho_{card} + (1+z)^3 \rho_0 (-w_m + n X_{ME})^n (1+w_m)))}{-(1+z)^{3(1+w_m)} \rho_0 + e^{X_{ME}} ((1+z)^{3(1+w_m)} \rho_0 + \rho_{card})} \quad (49)$$

and

$$w = \frac{w_m \rho_0 (1+z)^{3(1+w_m)} + (1+z)^{3w_m} (-(1+z)^3 \rho_0 w_m - e^{X_{ME}} ((1+z)^{-3w_m} \rho_{card} + (1+z)^3 \rho_0 (-w_m + n X_{ME})^n (1+w_m)))}{\rho_0 (1+z)^{3(1+w_m)} - (1+z)^{3(1+w_m)} \rho_0 + e^{X_{ME}} ((1+z)^{3(1+w_m)} \rho_0 + \rho_{card})} \quad (50)$$

where

$$X_{ME} = \left(\frac{\alpha \rho_{card}}{(1+z)^{3(1+w_m)} \rho_0 + \rho_{card}} \right)^n$$

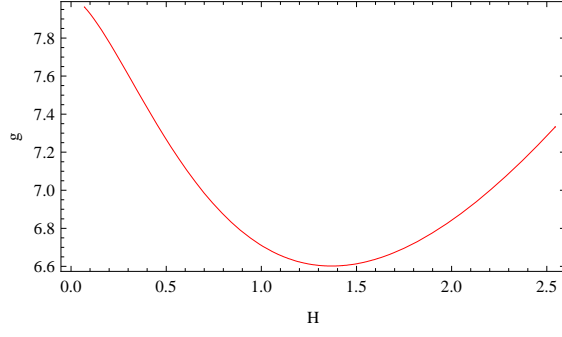


FIG. 21: The variation of w_c against H for $\alpha = 2.5$, $w_m = .01$, $n = .8$, $\rho_{card} = .1$, $\Lambda = .01$, $\rho_0 = .001$, $k = 1$, $l = .9$, $H_0 = 72$.

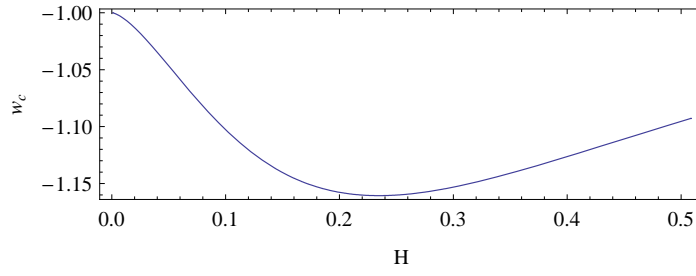


FIG. 22: The variation of w_c against H for $\alpha = 2.5$, $w_m = .01$, $n = .8$, $\rho_{card} = .1$, $\Lambda = .01$, $\rho_0 = .001$, $k = 1$, $l = .9$, $H_0 = 72$.

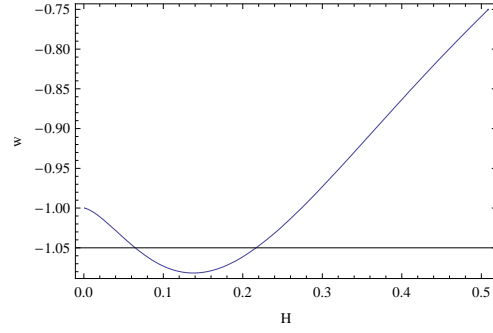


FIG. 23: The variation of w against H for $\alpha = 2.5$, $w_m = .01$, $n = .8$, $\rho_{card} = .1$, $\Lambda = .01$, $\rho_0 = .001$, $k = 1$, $l = .9$, $H_0 = 72$.

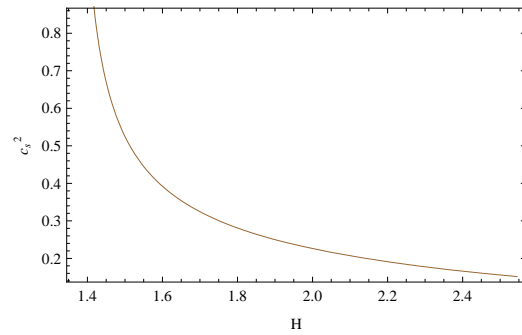


FIG. 24: The variation of c_s^2 against H for $\alpha = 2.5$, $w_m = .01$, $n = .8$, $\rho_{card} = .1$, $\Lambda = .01$, $\rho_0 = .001$, $k = 1$, $l = .9$, $H_0 = 72$.

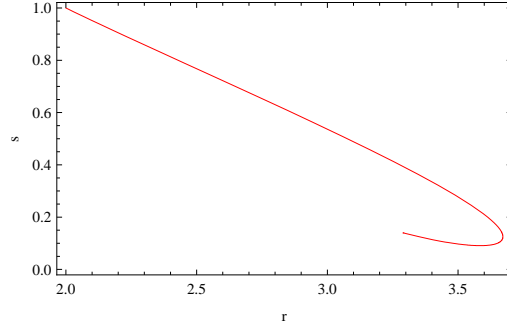


FIG. 25: The variation of s against r for $\alpha = 2.5, w_m = .01, n = .8, \rho_{card} = .1, \Lambda = .01, \rho_0 = .001, k = 1, l = .9, H_0 = 72$.

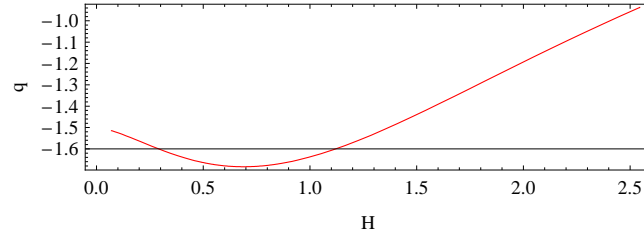


FIG. 26: The variation of q against H for $\alpha = 2.5, w_m = .01, n = .8, \rho_{card} = .1, \Lambda = .01, \rho_0 = .001, k = 1, l = .9, H_0 = 72$.

From (16), (18), (19), (20), (47) and (48) we get the statefinder parameters and deceleration parameter,

$$r = \frac{[2(1+z)^{-6w_m}\rho_{card}^2 + (1+z)^{3-3w_m}\rho_0\rho_{card}(4 - 9(-1 + nX_{ME})w_m(1 + w_m)) + (1+z)^6\rho_0^2(2 + 9w_m + 9(w_m^2 + n^2X_{ME}^2(1 + w_m)^2 + nX_{ME}(1 + w_m)(-1 + n + (-2 + n)w_m)))]}{[2(1+z)^{-3w_m}\rho_{card}^2 + 2(1+z)^3\rho_0]} \quad (51)$$

and

$$s = \frac{[2(1+z)^{-6w_m}\rho_{card}^2 + (1+z)^{3-3w_m}\rho_0\rho_{card}(2 + nX_{ME}(1 + w_m)(2 + 9w_m) - w_m(11 + 9w_m)) - (1+z)^6\rho_0^2(9n^2X_{ME}^2(1 + w_m)^2 + w_m(11 + 9w_m) + nX_{ME}(1 + w_m)(-11 + 9n + 9(-2 + n)w_m))]}{[(2((1+z)^3\rho_0 + (1+z)^{-3w_m}\rho_{card}))((1+z)^{-3w_m}\rho_{card} + (1+z)^3\rho_0(-w_m + nX_{ME}(1 + w_m)))]} \quad (52)$$

$$q = -\frac{2(1+z)^{-3w_m}\rho_{card} + (1+z)^3\rho_0(-1 - 3w_m + 3nX_{ME}(1 + w_m))}{2(1+z)^3\rho_0 + 2(1+z)^{-3w_m}\rho_{card}} \quad (53)$$

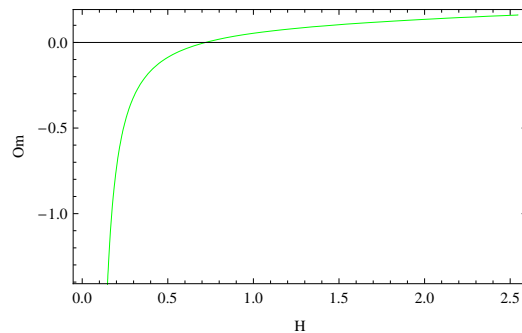


FIG. 27: The variation of Om against H for $\alpha = 2.5, w_m = .01, n = .8, \rho_{card} = .1, \Lambda = .01, \rho_0 = .001, k = 1, l = .9, H_0 = 72$.

Fig.21, 22 and 23 represents the variation of g , w_c and w against H respectively. From (9), (10), (16), (47) and (48) we plot the graph which shows the variation of the square of velocity of sound c_s^2 against H is given in Fig. 24, Fig.25 represents the variation of s against r and Fig.26 represents the variation of q against H . From (8), (21) and (46) we get the value of Om . Fig.27 represents the variation of Om against H . The values are taken as, $\alpha = 2.5$, $w_m = .01$, $n = .8$, $\rho_{card} = .1$, $\Lambda = .01$, $\rho_0 = .001$, $k = 1$, $l = .9$, $H_0 = 72$. From the figures, we see that g , w_c , w , q first decrease then increase and Om decreases as H decreases and c_s^2 lies between 0 and 1. The parameter s increases and keeps positive sign as r decreases.

V. DISCUSSIONS

In this work, the we have considered Cardassian Universe in Hořava-Lifshitz gravity. The energy density and pressure for Cardassian term have been found. Four types of Cardassian Universe models i.e., polytropic/power law, modified polytropic, exponential and modified exponential models have been considered for accelerating models. To investigate the natures of statefinder parameters, deceleration parameter, Om diagnostic and EoS parameters for all types of Cardassian models in Hořava-Lifshitz gravity, we have drawn all parameters w.r.t. Hubble parameters H .

In polytropic/power law Cardassian model of the universe g , w , q and Om parameters have been drawn in figures 1, 2, 5 and 6. We have seen that g , w , q and Om decrease as H decreases. The values are taken as, $w_m = .01$, $n = .5$, $\rho_{card} = .1$, $\Lambda = .01$, $\rho_0 = .001$, $k = 1$, $l = .9$, $H_0 = 72$. In this model, the EoS parameter w_c is constant. The variation of the square of velocity of sound c_s^2 against H is given in fig.3 and it has been observed that c_s^2 lies between 0 and 1. Also fig.4 represents the variation of s against r and the figure shows that s increases and keeps positive sign as r decreases from positive to negative values.

In modified polytropic Cardassian model of the universe g , w_c , w , q and Om parameters have been drawn in figures 7, 8, 9, 12 and 13. We have seen that g , w_c , w , q and Om decrease as H decreases. The values are taken as, $\alpha = .5$, $w_m = .01$, $n = .5$, $\rho_{card} = .1$, $\Lambda = .01$, $\rho_0 = .001$, $k = 1$, $l = .9$, $H_0 = 72$. The variation of the square of velocity of sound c_s^2 against H is given in fig.10 and it has been observed that c_s^2 lies between 0 and 1. Also fig.11 represents the variation of s against r and the figure shows that s increases and keeps positive sign as r decreases from positive to negative values.

In exponential Cardassian model of the universe g , w_c , w , q and Om parameters have been drawn in figures 14, 15, 16, 19 and 20. We have seen that g , w_c , w , q and Om decrease as H decreases. The values are taken as, $w_m = .01$, $n = 2$, $\rho_{card} = .1$, $\Lambda = .01$, $\rho_0 = .001$, $k = 1$, $l = .9$, $H_0 = 72$. The variation of the square of velocity of sound c_s^2 against H is given in fig.17 and it has been observed that c_s^2 lies between 0 and 1. Also fig.18 represents the variation of s against r and the figure shows that s increases and keeps negative sign as r decreases.

In modified exponential Cardassian model of the universe g , w_c , w , q and Om parameters have been drawn in figures 21, 22, 23, 26 and 27. We have seen that g , w_c , w , q first decrease then increase and Om decreases as H decreases. The values are taken as, $\alpha = 2.5$, $w_m = .01$, $n = .8$, $\rho_{card} = .1$, $\Lambda = .01$, $\rho_0 = .001$, $k = 1$, $l = .9$, $H_0 = 72$. The variation of the square of velocity of sound c_s^2 against H is given in fig.24 and it has been observed that c_s^2 lies between 0 and 1. Also fig.25 represents the variation of s against r and the figure shows that s increases and keeps positive sign as r decreases.

Acknowledgement:

The authors are thankful to IUCAA, Pune, India for warm hospitality where part of the work was carried out.

References:

- [1] A. Riess, et al., Astron. J. 116 (1998) 1009.
- [2] S. J. Perlmutter, et al., Astrophys. J. 517 (1999) 565.
- [3] J. L. Tonry, et al., Astrophys. J. 594 (2003) 1.
- [4] B. Barris, et al., Astrophys. J. 602 (2004) 571.
- [5] R. Knop, et al., Astrophys. J. 598 (2003) 102.
- [6] A.G. Riess, et al., Astrophys. J. 607 (2004) 665.

- [7] P. Astier, et al., *Astron. Astrophys.* 447 (2006) 31.
- [8] P. J. Steinhardt, L. Wang and I. Zlater, *Phys. Rev. D* 59(1999) 123504.
- [9] X. Z. Li, J. G. Hao and D. J. Liu, *Class. Quant. Grav.* 19 (2002) 6049.
- [10] D. J. Liu and X. Z. Li, *Phys. Lett. B* 611 (2005) 8.
- [11] K. Freese, F.C. Adams, J.A. Frieman, and E. Mottola, *Nucl. Phys. B* 287, 797(1987).
- [12] P.J.E. Peebles and B. Ratra, *Astrophys. J., Lett. Ed.* 325, L17(1988).
- [13] B. Ratra and P.J.E. Peebles, *Phys. Rev. D* 37, 3406(1988).
- [14] J. Frieman, C. Hill, A. Stebbins, and I. Waga, *Phys. Rev. Lett.* 75, 2077(1995).
- [15] L. Wang and P. Steinhardt, *Astrophys. J.* 508, 483(1998).
- [16] R. Caldwell, R. Dave, and P. Steinhardt, *Phys. Rev. Lett.* 80, 1582(1998).
- [17] G. Huey, L. Wang, R. Dave, R. Caldwell, and P. Steinhardt, *Phys. Rev. D* 59, 063005(1999).
- [18] C. Deffayet, *Phys. Lett. B* 502, 199(2001).
- [19] C. Deffayet, G. Dvali, and G. Gabadadze, *Phys. Rev. D* 65, 044023(2002).
- [20] C.B. Netterfield et al, *Astrophys. J.* 571 (2002) 604.
- [21] R. Stompor et al, *Astrophys. J.* 561 (2001) L7.
- [22] K. Freese, M. Lewis, *Phys. Lett. B* 540 (2002)1.
- [23] K. Freese, *New Astron. Rev.* 49 (2005) 103; *Nucl. Phys. (Proc. Suppl.)* 124 50 (2003).
- [24] R. Lazkoz, G. Len, *Phys. Rev. D* 71 (2005) 123516.
- [25] Y. Wang, K. Freese, P. Gondolo, M. Lewis, *Astrophys. J.* 594(2003) 25.
- [26] D. J. Liu, C. B. Sun and X. Z. Li, *Phys. Lett. B* 634, 442 (2006).
- [27] C. Pryke et al, *Astrophys. J.* 568, 46 (2002); N.W. Halverson et al, *Astrophys. J.* 568 (2002) 38.
- [28] P. Hořava, *JHEP* 0903 020 (2009).
- [29] P. Hořava, *Phys. Rev. D* 79 084008 (2009).
- [30] E. M. Lifshitz, *Zh. Eksp. Teor. Fiz.* 11 255 (1949).
- [31] R. G. Cai et al, *Phys. Rev. D* 80 041501 (2009).
- [32] G. Calcagni, *JHEP* 0909 112 (2009).
- [33] H. Lu et al, *Phys. Rev. Lett.* 103 091301 (2009).
- [34] V. Sahni, T. D. Saini, A. A. Starobinsky, and U. Alam, *JETP Lett.* 77, 201 (2003).
- [35] V. Sahni, A. Shafeloo and A. A. Starobinsky, *Phys. Rev. D* 78, 103502 (2008).
- [36] J. Lu, L. Xu, Y. Gui and B. Chang, arXiv:0812.2074v2 [astro-ph];
- [37] R. L. Arnowitt, S. Deser and C. W. Misner, *The Dynamics of General Relativity* appeared as Chapter 7, pp. 227-264, in *gravitation: an introduction to current research*, L. Witten, ed. (Wiley, New York, 1962), arXiv: gr-qc/0405109.
- [38] C. Charmousis, G. Niz, A. Padilla and P. M. Saffin, *JHEP* **0908** 070 (2009); T. P. Sotiriou, M. Visser and S. Weinfurtner, *JHEP* 0910 (2009) 033; C. Bogdanos and E. N. Saridakis, *Class. Quant. Grav.* **27** 075005 (2010).